Original Article

Open Access

Nonlinear adaptive control law design using TSMC for nuclear reactor in load following operation

Hamza Boubacar Kirgni*, Abdou Salam Bako Yahaya, Abdoul Razak Lasseini Gonga Yahaya, Ayouba Moussa Hassane

High Authority of Niger Atomic Energy (HANEA), Niger

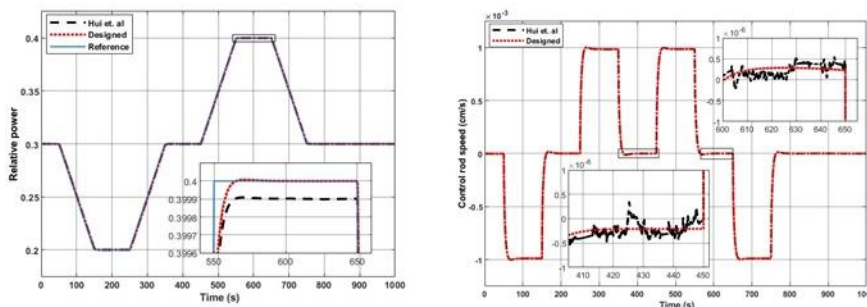** Corresponding author.*   E-mail address: h.boubacarkirgni.1783@gmail.com

ABSTRACT

The load-following process plays a crucial role within nuclear reactors. However, various factors, including uncertainties, can lead to performance degradation in these reactors. To address this, we propose a novel approach using nonlinear adaptive-based terminal sliding mode control (TSMC). To that purpose, the reactor nonlinear model is transformed to normal form using the feedback linearization technique. Based on that model and using the backstepping approach, a nonlinear nominal control law is constructed, which is then mounted with the adaptive discontinuous control law designed by TSMC. Then, a control law for the entire closed-loop system is developed to offer not only local asymptotic stability, but also resilience against uncertainty. A nonlinear terminal integral sliding surface is defined to solve the problem of SMC singularity. The system's stability was investigated using Lyapunov synthesis. To test the performance of the designed control law, numerical simulations are performed. The simulation results demonstrate that the designed control rule permits load-following control in addition to being insensitive to uncertainty.

Keywords: Feedback linearization; TSMC; Load-following; Power level.

Graphical abstract

1.   Introduction

Because of the present trend toward sustainable development, as well as its impact on the energy sector, the production of nuclear-based power has been brought into consideration [1]. However, besides its tarnished image, nuclear energy is still perceived as a durable platform to deal with the paradigms of reliable and clean energy. As a result of the Fukushima incident, the safety and stability of plant operations have received special attention. The power-level control approach is one of the most significant strategies for ensuring the plant's stability, safety, and efficiency [2]. However, given the increasing proportion of nuclear power in the electric grid, it is unavoidable to shift from the base-load process to the load-following process so that nuclear power can quickly meet the power demand from the electric network. Furthermore, nuclear reactor dynamics are characterized by significant nonlinearity and uncertainty caused by power changes, unmodeled dynamics, and external signals. As a result, these variables greatly reduce the system's control performance [3]. Furthermore, the reactor core reactivity fluctuates with fuel burnup, resulting in system performance degradation [4]. With all of this in mind, it is difficult to accomplish efficient reactor power level management throughout the load process.

Many studies have been conducted in the area of power level regulation since it is a key component in guaranteeing the stability, safety, and efficient operation of NPPs. Numerous effective control strategies have been put forth by researchers thus far. Li et al. [5] developed an H_∞ loop shaping controller for a linearized multivariable reactor core coordinated control system. In Ref. [6], Yan et al. introduced an H_∞ mixed sensitivity method to a small pressurized water reactor (SPWR). Dong [7] designed an adaptive power-level control method for nonlinear modular high-temperature gas-cooled reactor cores. Etchepareborda and Lolich [8] suggested a power-level control technique for pressurized water reactors based on nonlinear MPC (NMPC). Similarly, [9] gave a power-level control approach based on MPC for a transportable nuclear power station. Guoxu et al. (2016) [10] proposed a state-space MPC technique for PWR core power level regulation.

Soft-computing-based control techniques have the potential to improve a system's dynamic responsiveness. As a result, they were employed to regulate the reactor's power level. Khajavi et al. [11] developed a self-tuning robust optimum neural network control (NNC) law for nuclear reactors under load following operation. Alibeik [12] proposed an adaptive neural network control law for the core power of a pressurized water reactor. Dong [13] devised a nonlinear adaptive state observer for pressurized water reactors based on a neural network. In addition, [14] provided an MLP-compensated PD power-level control rule defined by an experientially-tuned PD regulator to assure constrained stability of the closed-loop based on the strong approximation ability of the multi-layer perceptron (MLP) artificial neural network. Furthermore, a genetic algorithm (GA) was used to improve the parameters of a control law. Mousakazemi et al. (2018) [15] reported a proportional integral and derivative (PID) control rule for reactor core power-level regulation, in which the PID gains were optimized and scheduled using a real-coded genetic algorithm (GA).

SMC is a robust nonlinear control method that is efficient. This technique has been widely used by control design academics due to its efficacy in dealing with uncertainty. Ansafari and Saadatzi [16] proposed an SMC system for nuclear reactor load-following operations to keep xenon oscillations within bounds. Hui et al. (2021) [17] recently designed a chattering-free higher-order sliding mode controller for a pressurized water reactor (PWR). In addition, Vajpayee [18] and Abdulraheem [19] conceived a hybrid control method for PWR by combining an optimal control strategy with integral sliding mode control. However, singularity constitutes one of the main drawbacks of SMC technique. Furthermore, while the system states might approach the equilibrium point, the convergence in conventional SMC does not occur in a finite period [20]. Towards this end, terminal sliding-mode control (TSMC), whose characteristics are higher control precision, faster, finite-time convergence [21] is proposed.

Since the dynamic of a nuclear reactor is subject to uncertainties, it is relevant to design a power level control law for ensuring not only the stability of the closed-loop system, but also its robustness against the uncertainties. In this paper, a nonlinear adaptive based-SMC control law is designed. The control law thus designed, incorporates a nominal control law devised by using feedback linearization with TSMC law.

The rest of the paper is arranged as follows. Section 1 develops the nonlinear mathematical model of the nuclear reactor. Section 3 enacts the nominal control law's design. Section 3 deals the adaptive based-SMC. Section 5 provides an observer design. Section 6 discusses the stability analysis. Section 7 contains numerical simulations and a discussion of the efficacy of the developed control law. Section 8 ends with conclusions.

2. Nuclear reactor core mathematical model

Nonlinear equations that show variations in power level, fuel and coolant temperatures, as well as time, are typically used to describe the dynamical model of the reactor core. In this work, nonlinear simulation, verification, and control law design are performed using the point kinetics equations. The model is coupled with one equivalent group of delayed neutron and reactivity feedback due to the lumped fuel and coolant temperatures. The point kinetic model is provided as [14], [22-23]:

$$
\begin{cases}
\dot{n}_r = \dfrac{\rho - \beta}{\Lambda} n_r + \dfrac{\beta}{\Lambda} C_r \\[2mm]
\dot{C}_r = \lambda n_r - \lambda C_r \\[2mm]
\dot{T}_f = \dfrac{\varepsilon_f P_0}{\mu_f} n_r - \dfrac{\Omega}{\mu_f} T_f + \dfrac{\Omega}{2\mu_f} T_o + \dfrac{\Omega}{2\mu_f} T_e \\[2mm]
\dot{T}_o = \dfrac{(1 - \varepsilon_f) P_0}{\mu_c} n_r + \dfrac{\Omega}{\mu_c} T_f - \dfrac{(2M + \Omega)}{2\mu_c} T_o + \dfrac{(2M - \Omega)}{2\mu_c} T_e \\[2mm]
\rho = \alpha_f (T_f - T_{f,m}) + \dfrac{\alpha_c}{2} (T_o - T_{o,m}) + \dfrac{\alpha_c}{2} (T_e - T_{e,m}) + \rho_r \\[2mm]
\dot{\rho}_r = G_r Z_r
\end{cases}
\tag{1}
$$

where n_r is the relative nuclear power, μ_c is the total heat capacity of the coolant inside the reactor core, C_r is the relative concentration of the delayed neutron precursor, M is the mass flow rate multiplied by heat capacity of the coolant, β is the fraction of delayed neutrons, T_f is the average fuel temperature, Λ is the effective prompt neutron lifetime, Ω is the heat transfer coefficient between fuel and coolant, λ is the radioactive decay constant of delayed neutron precursor, ε_f is fraction of reactor power deposited in the fuel, P_0 is the rated reactor thermal power, α_f and α_c are respectively the reactivity coefficients of the fuel and coolant temperatures, T_o is the average coolant temperature of the reactor core, T_e is temperature of the water entering the reactor, μ_f is the total heat capacity of the fuel elements, G_r is the differential reactivity worth of the control rod, Z_r is the control input, control rod speed in units of fraction of core length per second, and ρ is the total reactivity.

Let introduce
$$
\begin{cases}
\delta n_r = n_r - n_{r0} \\
\delta C_r = C_r - C_{r0} \\
\delta T_f = T_f - T_{f0} \\
\delta T_o = T_o - T_{o0} \\
\delta T_e = T_e - T_{e0} \\
\delta \rho_r = \rho_r - \rho_{r0}
\end{cases}
\tag{2}
$$

with $\delta n_r, \delta C_r, \delta T_f, \delta T_o, \delta T_e$, and $\delta \rho_r$ the deviation of the actual values of n_r, C_r, T_f, T_o, T_e and ρ_r from their equilibrium values $n_{r0}, C_{r0}, T_{f0}, T_{o0}, T_{e0}$, and ρ_{r0} respectively.

Then combine (1) and (2), it results

$$
\begin{cases}
\delta \dot{n}_r = -\dfrac{\beta}{\Lambda} \delta n_r + \dfrac{\beta}{\Lambda} \delta C_r + \dfrac{\alpha_f n_r}{\Lambda} \delta T_f + \dfrac{\alpha_c n_r}{2\Lambda} \delta T_o + \dfrac{\alpha_c n_r}{2\Lambda} \delta T_e + \dfrac{n_r}{\Lambda} \delta \rho_r \\[2mm]
\delta \dot{C}_r = \lambda \delta n_r - \lambda \delta C_r \\[2mm]
\delta \dot{T}_f = \dfrac{\varepsilon_f P_0}{\mu_f} \delta n_r - \dfrac{\Omega}{\mu_f} \delta T_f + \dfrac{\Omega}{2\mu_f} T_o \\[2mm]
\delta \dot{T}_o = \dfrac{(1 - \varepsilon_f) P_0}{\mu_c} \delta n_r + \dfrac{\Omega}{\mu_c} \delta T_f - \dfrac{(2M + \Omega)}{2\mu_c} \delta T_o \\[2mm]
\delta \dot{\rho}_r = G Z_r
\end{cases}
\tag{3}
$$

It is relevant to point out that δT_e reflects the influence of the dynamic of the secondary loop to the primary loop, thus it is considered as uncertainty. In addition, the physical parameters such as $\mu_c, \Omega, M, \alpha_f$ and α_C result in uncertainties as they depend on the power level.

For reasons of simplicity, we define $[x_{i(i=1,\ldots,4)}] = [\delta n_r, \delta C_r, \delta T_f, \delta T_o]$ and assume that the uncertainty is bounded, i.e., $\|\delta T_e\| \leq w_1$.

3. Nominal control law design

Let's regard ξ_r as virtual input to system (3), then consider the following nonlinear system

$$\dot{x} = f(x) + g(x)\xi$$
$$y = h(x) \tag{4}$$

where x is the state vector, $f(x)$, $g(x)$ and $h(x)$ are smooth vector functions and ξ is the nominal control input. Suppose that the system (4) is rewritten into normal form as follows [24]

$$\dot{v}_1 = v_2$$
$$\dot{v}_2 = v_3$$
$$\vdots$$
$$\dot{v}_r = v_{r+1}$$
$$\dot{v}_{r+1} = \alpha(v,\mu) + \beta(v,\mu)\xi_{rn}$$
$$\dot{\mu} = z(v,\mu)$$
$$y = v_2 \tag{5}$$

where r is the relative degree, $\alpha(v,\mu)$ and $z(v,\mu)$ are smooth vector functions, and $\beta(v,\mu)$ nonsingular vector function for all $[v^T \mu^T]^T$

Assumptions:

It is assumed that:

- The zero-dynamics related to the nonlinear system (4) is stable.
- The vector functions $\alpha(v,\mu) = L_f^r h(x)$ and $\beta(v,\mu) = L_g L_f^{r-1} h(x)$, where $L_p h(x) = \frac{\partial h(x)}{\partial x}.p$, are locally Lipschitz in the domain containing the origin.

Then, the nominal control law that locally asymptotically stabilizes the system is given by

$$\xi_{rn} = -\frac{1}{\beta(v,\mu)}\left(\alpha(v,\mu) + \sigma_1 e + \sigma_2 \int_0^t e d\tau - \dot{y}_d\right) \tag{6}$$

where $e = y - y_d$ is the tracking error, y_d is the reference input and the coefficients $\sigma_{1,2}$ are selected such that the polynomial

$$P(s) = s^2 + \sigma_1 s + \sigma_0 \tag{7}$$

is Hurwitz.

4. Adaptive-based sliding mode control design

Assume that the nonlinear system (4) is subject to uncertainties (including both output and input uncertainties) and is given by

$$\dot{x} = f(x) + g(x)\xi + \varphi(t)$$
$$y = h(x) \tag{8}$$

where $\varphi(t)$ denotes the uncertainties and it supposes to be bounded, i.e., $\|\varphi(t)\| \leq \varphi_1$.

Then, the control objective is to design a referenced control input ξ_r enables to stabilize the system (8) in the presence of both matched and output uncertainties. In this section, an adaptive control law-based sliding mode is designed to compensate for the negative influences due to the uncertainties. Thus, the reference control input be given by

$$\xi_r = \xi_{nr} + \xi_{sar} \qquad (9)$$

where ξ_{nr} is the nominal control law and ξ_{sar} is the adaptive control law.

Typically, the design of a sliding mode control law is performed into two steps. First, a suitable sliding surface should be designed so as to constrain the system dynamics to the sliding manifold to guarantee a good tracking performance. Second, discontinuous control law is then devised to not only force the system trajectory to the sliding surface but also retained there once it is reached. In SMC, the design of an appropriate switching surface is characterized by solving the problem of existence, while reaching and subsequently maintaining the system states on the sliding surface is achieved by solving the reachability problem [25]. Hence, let define a nonlinear integral terminal sliding surface as

$$s = Gz^a \qquad (10)$$

with

$$z = s_1 - \int_0^t \dot{s}_{1n} d\tau \ ; \ a \in \mathbb{N}^* \ and \ G > 0 \qquad (11)$$

where $e = y - y_d$ and $e_n = y_n - y_d$ correspond respectively to the system tracking error and the nominal system tracking error, and y_d is the reference input.

Then, we get the following theorem.

Theorem 1: Consider the output-dependent integral sliding surface (10) and assume that the reference control input is provided by (9) where the adaptive control law is given by

$$\xi_{sar} = -\widehat{K} sign(s) \qquad (12)$$

and $\widehat{K}$ provides the estimation of the upper bound value of the uncertainties as

$$\widehat{K} = \mathcal{E}aza - 1|s| \qquad (13)$$

then, the closed-loop system (8) and (9) is locally asymptotically stable in the presence of the uncertainties.

Proof:

In order to assess the stability of the system, a functional Lyapunov candidate is selected as

$$V_1 = \frac{1}{2G} s^2 + \frac{1}{2\delta} \widetilde{K}^2 \qquad (14)$$

with $\widetilde{K} = \widehat{K} - K$ and $\delta > 0$.

Taking the time derivative of V_1 yields

$$\dot{V}_1 = \frac{1}{G} s\dot{s} + \frac{1}{\delta} \widetilde{K}\dot{\widetilde{K}} \qquad (15)$$

During sliding mode, the tracking error of the system is equal to that of the nominal system. In other words, the output of the system follows that of nominal system. Hence, we have

$$\dot{V}_1 = saz^{a-1}\left(-\frac{\beta}{\Lambda}x_1 + \frac{\beta}{\Lambda}x_2 + \frac{\alpha_f n_r}{\Lambda}x_3 + \frac{\alpha_c n_r}{2\Lambda}x_4 + \varphi + \frac{n_r}{\Lambda}x_5 - y_d - \left(-\frac{\beta}{\Lambda}x_1 + \frac{\beta}{\Lambda}x_2 + \frac{\alpha_f n_r}{\Lambda}x_3 + \frac{\alpha_c n_r}{2\Lambda}x_4 + \frac{n_r}{\Lambda}x_5 - y_d\right)\right) + \frac{1}{\delta}\tilde{K}\dot{\tilde{K}}$$

$$= saz^{a-1}(\varphi + u_{sa}) + \frac{1}{\delta}\tilde{K}\dot{\tilde{K}} = -az^{a-1}\hat{K}|s| + az^{a-1}s\varphi + \frac{1}{\delta}(\hat{K} - K)\mathcal{E}az^{a-1}|s|$$

$$\leq -a|z^{a-1}|\hat{K}|s| + a|z^{a-1}||s|\|\varphi\| + \frac{1}{\delta}(\hat{K} - K)\mathcal{E}a|z^{a-1}||s| \leq a|z^{a-1}||s|\left(-(\hat{K} - \varphi_1) + \frac{1}{\delta}(\hat{K} - K)\mathcal{E}\right)$$

$$\leq a|z^{a-1}||s|\left(-(\hat{K} - \varphi_1) + \frac{1}{\delta}(\hat{K} - K)\mathcal{E} + K - K\right) \leq a|z^{a-1}||s|\left(-(\hat{K} - K) + \frac{1}{\delta}(\hat{K} - K)\mathcal{E} - (K - \varphi_1)\right)$$

$$\leq a|z^{a-1}||s|\left(-(\hat{K} - K)\left(1 - \frac{1}{\delta}\mathcal{E}\right) - (K - \varphi_1)\right)$$

$$\leq a|z^{a-1}|\left(-(\hat{K} - K)\left(|s| - \frac{1}{\delta}\mathcal{E}|s|\right) - (K - \varphi_1)|s|\right) \tag{16}$$

Then, choose

$$a_1 = a|z^{a-1}|(K - \varphi_1) \tag{17}$$

$$a_2 = a|z^{a-1}|\left(|s| - \frac{1}{\delta}\mathcal{E}|s|\right) \tag{18}$$

$$a = a_1/a_2 \tag{19}$$

it yields

$$\dot{V}_1 \leq -a_1|s| - a_2(\hat{K} - K) \leq -a_1\sqrt{2G}|s|/\sqrt{2G} - a_2\sqrt{2\delta}(\hat{K} - K)/\sqrt{2\delta} \leq -\min\left(a_1\sqrt{2G}, a_2\sqrt{2\delta}\right)\left(\frac{|s|}{\sqrt{2G}} + \frac{\tilde{K}}{\sqrt{2\delta}}\right)$$

$$\leq -a_3 V_1^{\frac{1}{2}} \tag{20}$$

with $a_3 = min\left(a_1\sqrt{2G}, a_2\sqrt{2\delta}\right) > 0$. The above inequality holds for any $a_1 > 0$, $a_2 > 0$, i.e., for $K > \varphi_1$ and $\mathcal{E} > \delta$. This completes the proof.

In the following a control law that stabilizes the entire system is derived. Indeed, the virtual control input (9) simply gives the referenced value of ξ, i.e., the reactivity which must be produced by the control rods.

Theorem 2: Suppose that the control input is given by

$$u = \dot{\xi}_r - k_\xi x_1 \tag{21}$$

where $k_\xi > 0$ is a tuning gain and ξ_r is provided by (9), then the local asymptotic stability of the entire system (3) can be guaranteed by the control input (21).

Proof:

Let us select a new Lyapunov function as

$$V_2 = V_1 + \frac{1}{2}e_\xi^2 \tag{22}$$

where V_1 is given by (14), and $e_\xi = \xi - \xi_r$.

Differentiate V_2 through the trajectory provided by (8) gives

$$\dot{V}_2 = \dot{V}_1 + e_\xi \dot{e}_\xi = \dot{V}_1 + k_\xi e_\xi(\dot{\xi} - \dot{\xi}_r) \leq -a_1|s| - a_2(\hat{K} - K) - k_\xi|e_\xi||x_1| \leq \frac{-a_1\sqrt{2G}|s|}{\sqrt{2G}} - \frac{a_2\sqrt{2\delta}(\hat{K} - K)}{\sqrt{2\delta}} - \frac{k_\xi\sqrt{2}|e_\xi||x_1|}{\sqrt{2}}$$

$$\leq -\min\left(a_1, a_2, k_\xi\sqrt{2}\right)\left(\frac{|s|}{\sqrt{2G}} + \frac{\tilde{K}}{\sqrt{2\delta}} + \frac{|e_\xi|}{\sqrt{2}}\right) \leq -a_4 V_2^{\frac{1}{2}} \tag{23}$$

with $a_4 = \min\left(a_1, a_2, k_\xi\sqrt{2}\right)$. This completes the proof.

5. Observer design

In nuclear reactor, the variations of the relative concentration of delayed neutron precursor x_2 and the average fuel temperature x_3 cannot be obtained directly, therefore an observer is indispensable for obtaining their estimation values. The following proposition gives an observer whose unique property is to provide an asymptotic convergence of the estimated values $\hat{x}_2$ and $\hat{x}_3$ to their actual values x_2 and x_3.

Proposition 1: Consider the following observer

$$\begin{cases} \dot{\hat{x}}_2 = \lambda x_1 - \lambda \hat{x}_2 \\ \dot{\hat{x}}_3 = \dfrac{\varepsilon_f P_0}{\mu_f} x_1 - \dfrac{\Omega}{\mu_f} \hat{x}_3 + \dfrac{\Omega}{2\mu_f} x_4 \end{cases} \qquad (24)$$

then, the estimated value $\hat{x}_{i,(i=2,3)}$ converges asymptotically to their actual value of $x_{i,(i=2,3)}$.

Proof:

Accordingly, the estimation error is defined as

$$\begin{cases} e_2 = x_2 - \hat{x}_2 \\ e_3 = x_3 - \hat{x}_3 \end{cases} \qquad (25)$$

Differentiate equation (25) w.r.t time gives

$$\begin{cases} \dot{e}_2 = -\lambda e_2 \\ \dot{e}_3 = -\dfrac{\Omega}{\mu_f} e_3 \end{cases} \qquad (26)$$

In order to assess the result's convergence of the observer, a Lyapunov function is chosen as

$$V_3 = \frac{1}{2} e_2^2 + \frac{1}{2} e_3^2 \qquad (27)$$

Then, take the time derivative of V_3 along the estimation error dynamics (26), gives

$$\dot{V}_3 = -\lambda e_2^2 - \frac{\Omega}{\mu_f} e_3^2 = -\frac{\sqrt{2}\lambda}{\sqrt{2}} e_2^2 - \frac{\sqrt{2}\Omega}{\mu_f \sqrt{2}} e_3^2 \le -\min\left(\sqrt{2}\lambda, \frac{\sqrt{2}\Omega}{\mu_f}\right)\left(\frac{1}{\sqrt{2}} e_2^2 + \frac{1}{\sqrt{2}} e_3^2\right) \le -a_5 V_3$$

$$\le -a_5 V_3^{\frac{1}{2}} \qquad (28)$$

with $a_5 = \min\left(\sqrt{2}\lambda, \frac{\sqrt{2}\Omega}{\mu_f}\right)$.

From inequality (28), one can conclude that the estimation error is bounded and the convergence of estimated states to their actual values is guaranteed.

6. Closed-Loop Stability analysis

In this section the stability of the of entire closed-loop system will be addressed. Thus, the control law to locally stabilize the whole system (3) is given by

$$u = \dot{\xi}_r - k_\xi x_1$$

$$\xi_r = -\frac{1}{\beta(v,\mu)}\left(\alpha(v,\mu) + \sigma_1 e + \sigma_2 \int_0^t e d\tau - \dot{y}_d\right) - \hat{K} sign(s)$$

$$\dot{\hat{K}} = \varepsilon a z^{a-1}|s|$$

$$\dot{\hat{x}}_2 = \lambda x_1 - \lambda \hat{x}_2$$

$$\dot{\hat{x}}_3 = \frac{\varepsilon_f P_0}{\mu_f} x_1 - \frac{\Omega}{\mu_f} \hat{x}_3 + \frac{\Omega}{2\mu_f} x_4 \quad (29)$$

Theorem 3: Consider the nonlinear adaptive-based sliding mode control law (13) and the sliding surface (10), then the local asymptotic stability of the entire closed-loop system formed by (3) and (29) is guaranteed. In addition, during sliding mode we have $e \to e_n$, i.e., $y \to y_n$.

Proof:

Let select a new Lyapunov function for the whole system

$$V = V_2 + V_3 \qquad (30)$$

where V_2 and V_3 are provided by (22) and (27) respectively.

The time derivative of V gives

$$\dot{V} = \dot{V}_2 + \dot{V}_3 \leq -a_1|s| - a_2(\hat{K} - K) - k_\xi|e_\xi||x_1| - \lambda e_2^2 - \frac{\Omega}{\mu_f}e_3^2$$

$$\leq \frac{-a_1\sqrt{2G}|s|}{\sqrt{2G}} - \frac{a_2\sqrt{2\delta}(\hat{K} - K)}{\sqrt{2\delta}} - \frac{k_\xi\sqrt{2}|e_\xi||x_1|}{\sqrt{2}} - \frac{\sqrt{2}\lambda}{\sqrt{2}}e_2^2 - \frac{\sqrt{2}\Omega}{\mu_f\sqrt{2}}e_3^2$$

$$\leq -\min\left(a_1, a_2, k_\xi\sqrt{2}, \sqrt{2}\lambda, \frac{\sqrt{2}\Omega}{\mu_f}\right)\left(\frac{|s|}{\sqrt{2G}} + \frac{\tilde{K}}{\sqrt{2\delta}} + \frac{|e_\xi|}{\sqrt{2}} + \frac{1}{\sqrt{2}}e_2 + \frac{1}{\sqrt{2}}e_3\right)$$

$$\leq -a_6 V^{\frac{1}{2}} \tag{31}$$

with $a_6 = min\left(a_1, a_2, k_\xi\sqrt{2}, \sqrt{2}\lambda, \frac{\sqrt{2}\Omega}{\mu_f}\right)$. This completes the proof.

From equation (30), one can conclude that the local asymptotic stability of the closed-loop system (3)-(29) is ensured.
Remarks:

- Due to the integral term in the sliding surface (11), the reaching phase is eliminated. Therefore, the control system robustness is improved.
- The adaptive gain (13) does not need the prior knowledge of the uncertainties.
- From equation (30) and (31), it can be seen that the dynamic performance of the system under the control law (29) is strengthened when the gain k_ξ is small enough.

7. Simulation

In this section, we examine the effectiveness of the nonlinear adaptive-based Sliding Mode Control (SMC) law (29), specifically in the context of controlling the power level of nuclear reactors during load-following transient operations. The control strategy developed herein is compared with two other methods: the Adaptive Second-Order Nonsingular Terminal Sliding Mode Power-Level Control for Nuclear Power Plants [26] and a Robust Optimal Control law [27]. The numerical simulation is carried out using the reactor nonlinear dynamical model (3). To avoid chattering, the saturation function "$sat(\cdot)$" is used instead of the signum function "$sign(\cdot)$" in the discontinuous control law (12) during the simulation. The matched as well as the output uncertainties are determined by the sum of the sigmoid and linear chirp signals, respectively as

$$w(t) = w_0\left(7sin(10^{-4}t) + 3sin(10^{-3}t) + 2sin(10^{-2}t) + sin(10^{-1}t)\right) \tag{32}$$
$$\vartheta(t) = \vartheta_0 sin(2\pi \times 10^{-4}t + 5\pi \times 10^{-6}t^2) \tag{33}$$

where $w_0 = 10^{-3}$ and $\vartheta_0 = 10^{-5}$ are magnitudes of disturbances and uncertainties

Here, the power demand corresponds to the set point which is provided by the reference input signal. Three loads following transient cases are studied. The power level control is driven by the error signal x_1 to provide a proper control rod speed so that the power output follows the set point. The technique of the power level control consists in inserting and withdrawing the control rod through the control rod speed to respectively decrease and increase the power level. It is worth noting that both the variation of the average temperature and the relative power are needed to drive the generation of the control rod speed signal. Thus, the closed-loop system reaches an equilibrium point when the reactivity generated by the feedback effect of the temperature compensates that induced by the control rods.

Figures 1 and 3 exhibit the performance of the designed control law for the first two load-following patterns with a set point given as: initially, the power is at 90% FFP; after 50sec it gradually increases up to 100% FFP where it is held for 100 sec; it then decreases progressively to reach its initial value; after 100sec it again decreases to 80% FFP and be maintained there for 100 sec; finally, it increases to attain its initial value where it is kept the remaining time and inversely for the second load-following pattern with power level of 30% FFP, 20% FFP and 40% FPP correspondingly. Figures 1.a and 3.a show the relative power of the reactor core. From these figures, it can be observed that, the power output tracks effectively the reference signal. Moreover, as shown from these figures, there are no overshoot and undershoot. Figures 1.b-c and 3.b-c demonstrate the reactivity induced by the control rod as well as the control rod speed respectively. As it can be seen, both the reactivity induced by the control rod and the control rod speed are at the same times smooth and at acceptable limits. Figures 1.d-e and 3.d-e illustrate the tracking error and the sliding surface. The adaptive gain $\hat{K}$ are represented in figures 1.f and 3.f. It is observed that for both cases the gain $\hat{K}$ increases gradually as time increases to compensate for the effect due to uncertainties. Thus, the designed control law is adaptive to the system uncertainties.
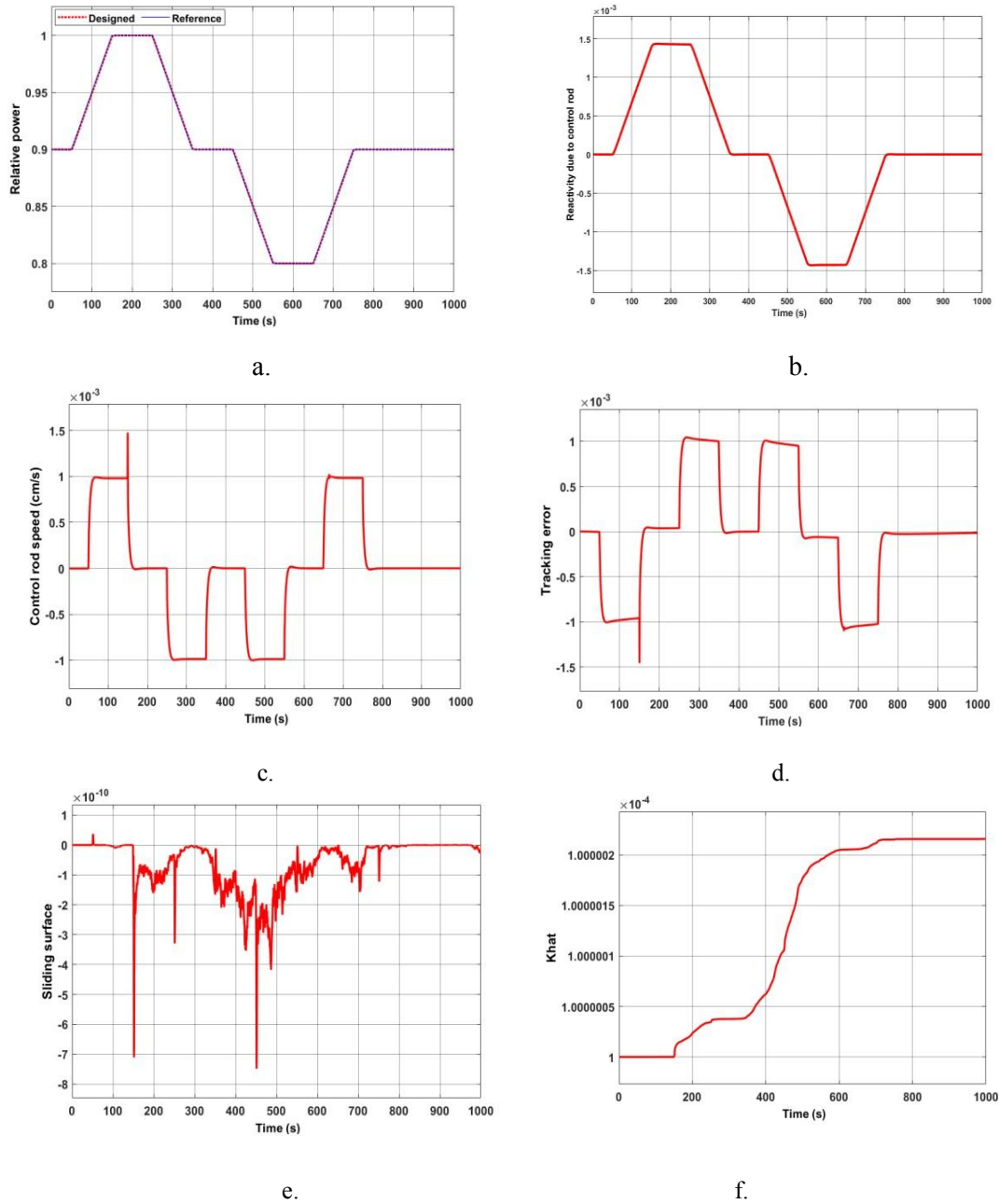
Figure 1: Performance of the designed control law in case 1.

The comparison of the designed control law with those devised in references [26] and [27] for the first two load-following patterns is shown in figures 2 and 4. From the aforementioned figures, it can be seen that the control law designed in this work presents better performances than those obtained [26] and [27]. Indeed, the designed control law is more robust against the negative influence due to the uncertainties and spends less control effort to stabilize the core power.

As for the case 2, the power is at 100% FFP for 50sec initially; it then continuously decreases till to 20% FFP and stays for 100sec; it increases to regain its initial value where it is held for rest of the time. The performance of the designed control law for this case are depicted in figure 5. Similarly, figure 5.a-f illustrate respectively the relative power, the reactivity induced by the control rod, the control rod speed, the tracking error, the sliding surface and the adaptive gain $\hat{K}$. Similar observations are found in this case as in previous one. Indeed, the relative power follows perfectly its reference signal. As for the total reactivity and the control rod speed, both are bounded and vary smoothly. Besides, the estimated gain $\hat{K}$ varies over time to give an estimation of the upper bound of the uncertainties.

Figure 6 compares the control law obtained in this work to those developed in [26] and [27]. Similarly, the control law proposed in this study has superior performances than the ones achieved in [26] and [27], as shown in the figure 6. The designed control law is able to cancel out both the input and output uncertainties. Finally, it can be concluded that the designed control law offers the system a high control performance during load-following process.
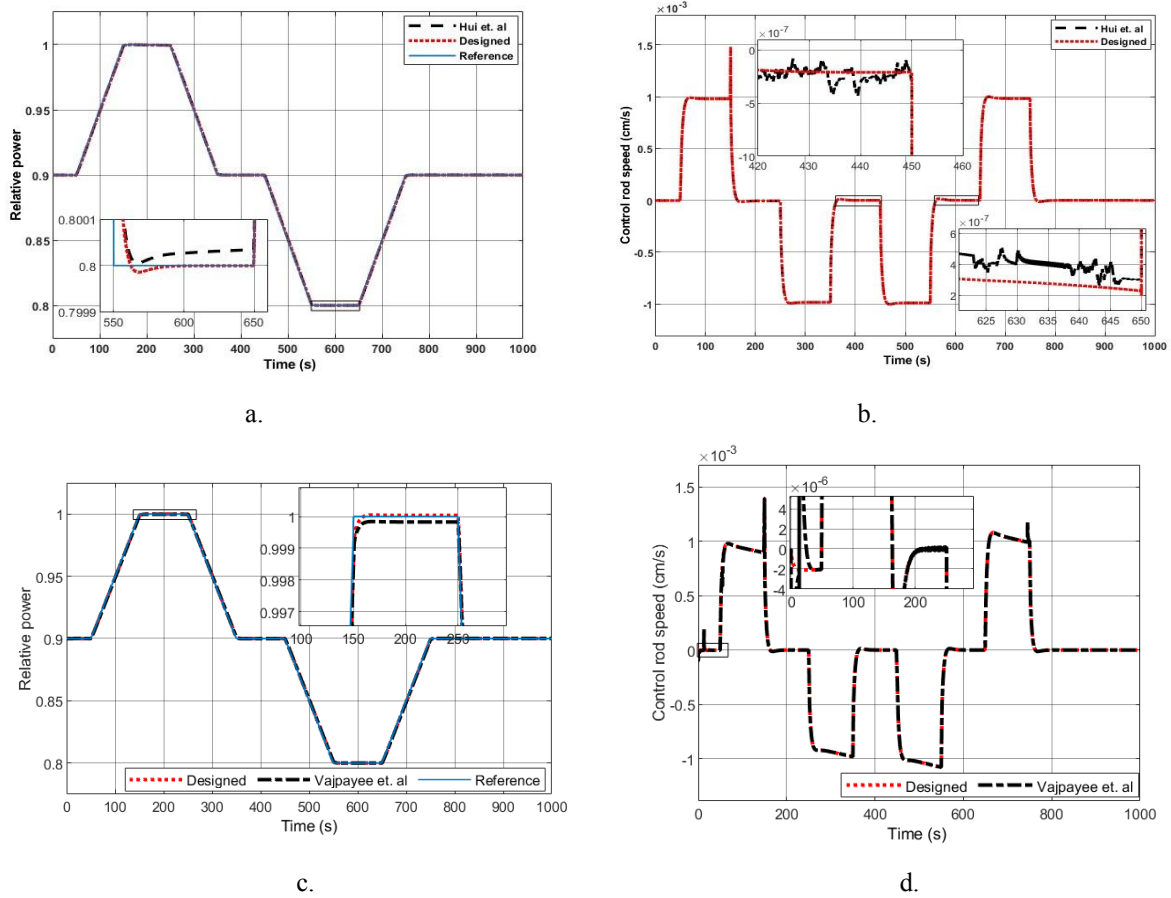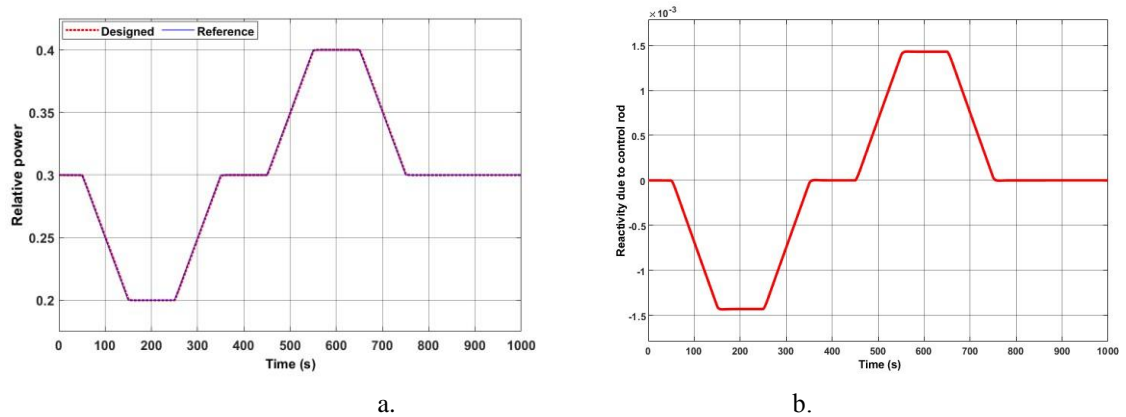

a.

b.
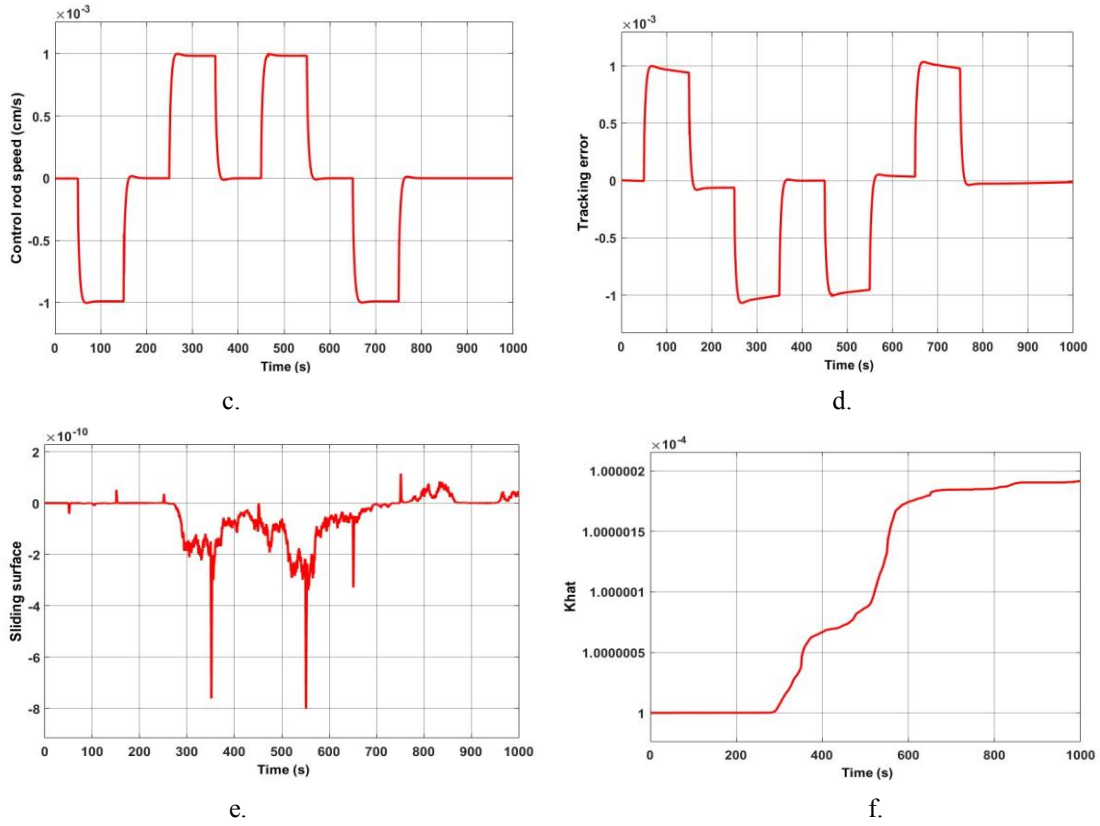

c.

d.

Figure 2. Comparison of the control laws in case 1.

a.

b.

Figure 3: Performance of the designed control law in case 2.

Figure 4. Comparison of the control laws in case 2.

a.

b.

c.

d.

e.
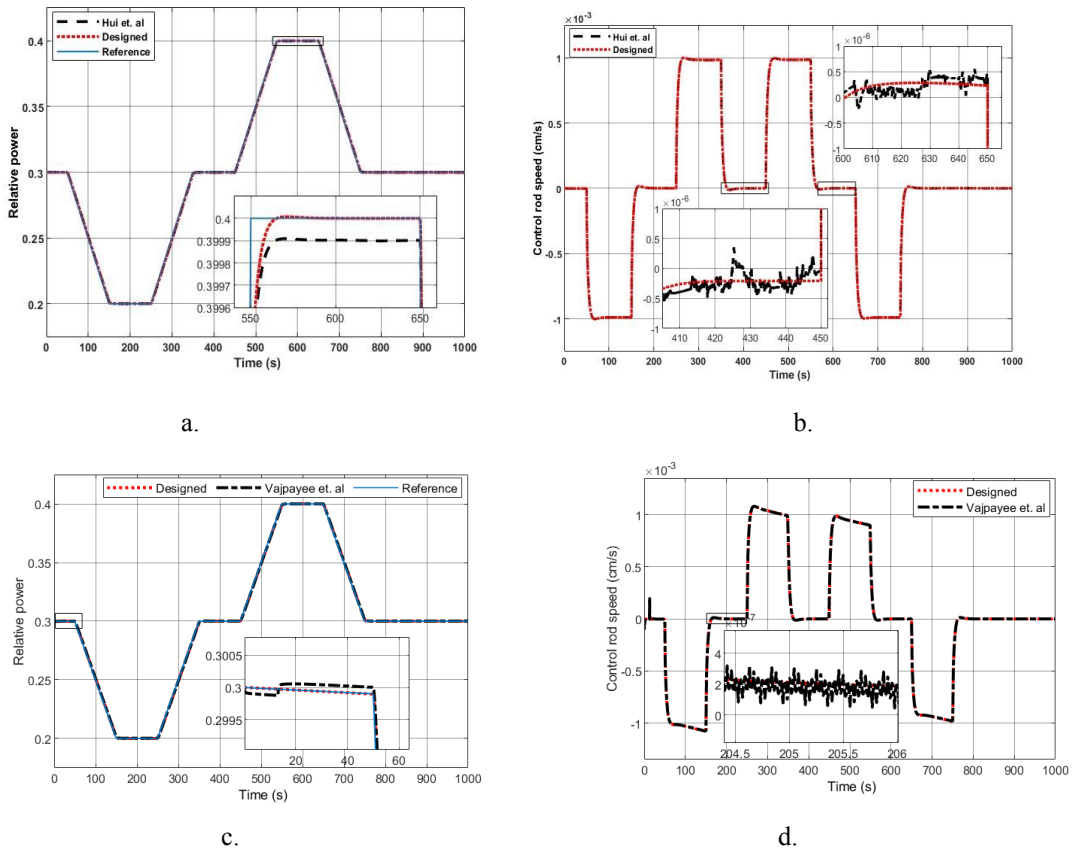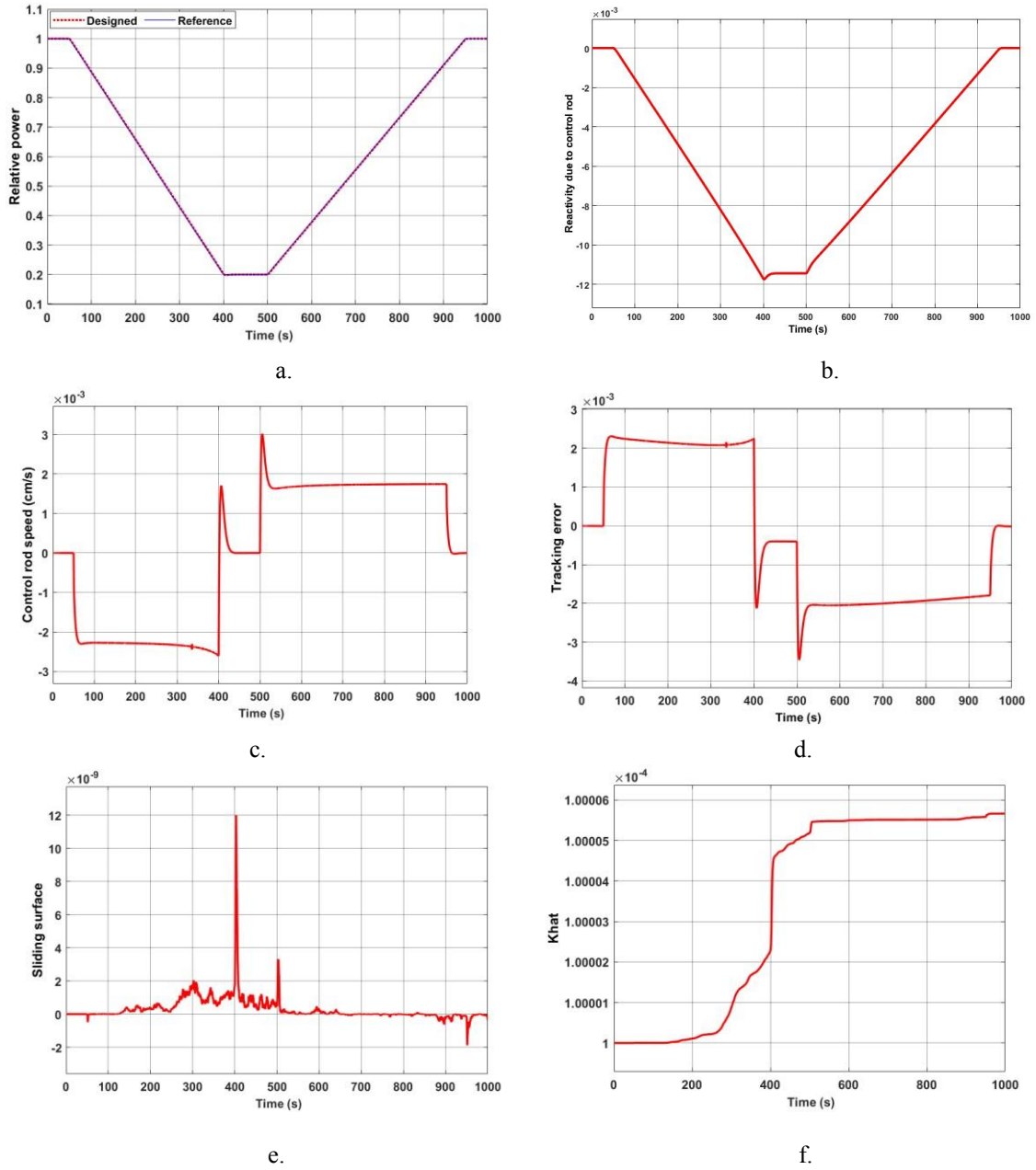

f.

Figure 5: Performance of the designed control law in case 3.

a.   b.

c.   d.
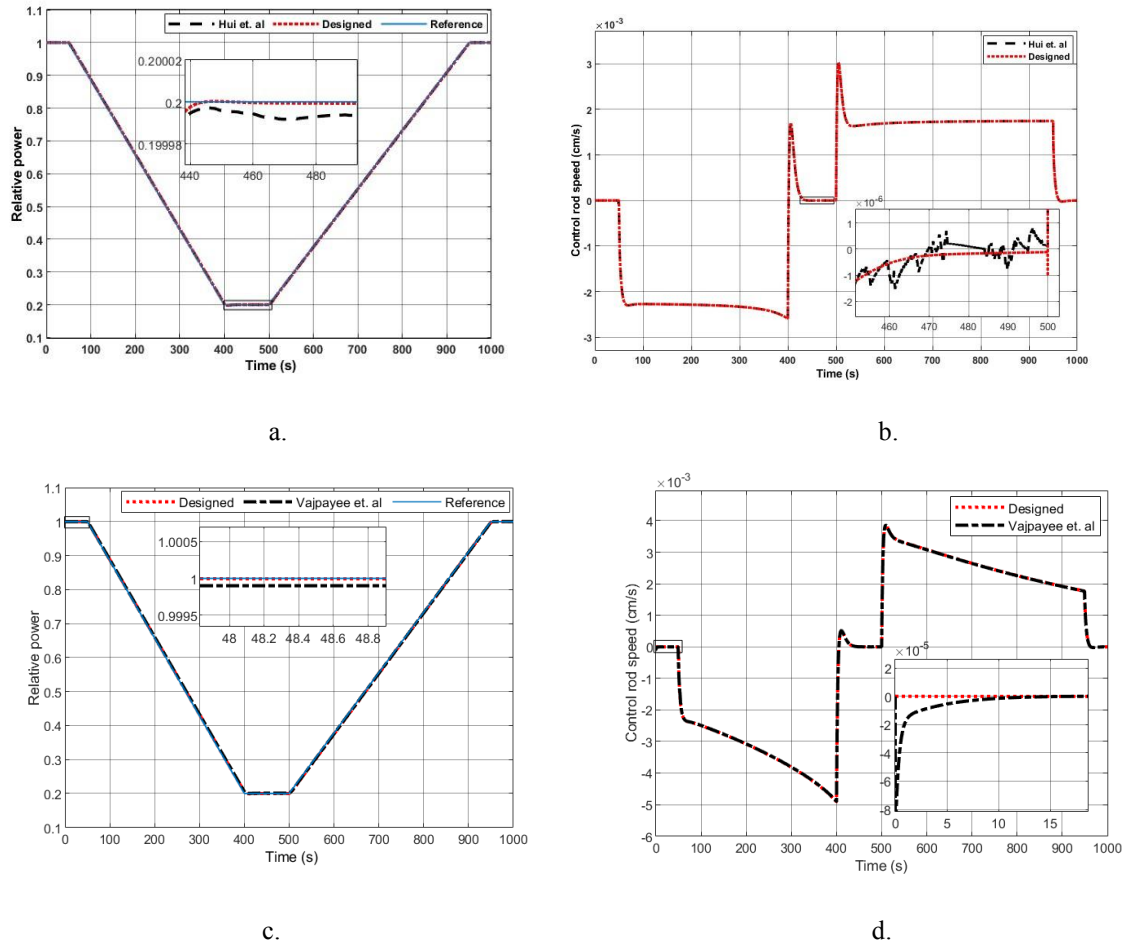
Figure 6. Comparison of the control laws in case 3.

8.   Conclusion

As nuclear energy continues to flourish, it is undeniable to guarantee the stability, the safety and the effective operation of nuclear reactors. Power level control technique is one way to ensure safe, stable and efficient operation of these reactors. In addition, due to the growing portion of nuclear power within the electric grid, load-following process is indispensable to meet the power demand. Hence, in this regard, a nonlinear adaptive based TSMC is presented in this paper for reactor core power control during load following operation. It was proved that this adaptive control law cannot only guarantee the local asymptotic stability of the closed-loop system, but also achieves a remarkable control performance during load following operation in the presence of varying uncertainties. The problem singularity associated with the SMC has been addressed by defined a nonlinear terminal sliding surface. The stability of the system has been analysed by using of Lyapunov theory. And finally, numerical simulations have been conducted to check the exactitude of the theoretical results. Moreover, the designed control law has been compared with that acquired in the references [26] and [27]. It follows from the comparison that the control law obtained in this work performs well than the ones devised in [26] and [27].

Funding Support

This research received no external funding.

Ethical Statement

This study does not contain any studies with human or animal subjects performed by any of the authors.

Conflict of Interest

The authors declare that they have no conflict of interest.

Data Availability Statement

Not applicable.

References

1. Brook BW, Alonso A, Meneley DA, Misak J, Blees T, van Erp JB. Why nuclear energy is sustainable and has to be part of the energy mix. *Sustainable Materials and Technologies*. 2014 Dec;1:8–16. https://doi.org/10.1016/j.susmat.2014.11.001
2. Dong Z. Nonlinear adaptive power-level control for modular high temperature gas-cooled reactors. *IEEE Transactions on Nuclear Science*. 2013;60(2):1332–45. https://doi.org/10.1109/TNS.2013.2252023
3. Chengbo Y, Wang J, Xiuchun L, Jie Z, Zhida Y. Load-following control of nuclear reactors based on l1 adaptive algorithm. In: Proceedings of the 2018 13th World Congress on Intelligent Control and Automation; July 4-8, 2018; Changsha, China.
4. Eliasi H, Menhaj MB, Davilu H. Robust nonlinear model predictive control for a PWR nuclear power plant. *Progress in Nuclear Energy*. 2012 Jan;54(1):177–85. https://doi.org/10.1016/j.pnucene.2011.06.004
5. Li G, Liang B, Wang X, Li X. Multivariable modeling and nonlinear coordination control of nuclear reactor cores with/without xenon oscillation using H∞ loop shaping approach. *Annals of Nuclear Energy*. 2018 Jan;111:82–100. https://doi.org/10.1016/j.anucene.2017.08.027
6. Yan X, Wang P, Qing J, Wu S, Zhao F. Robust power control design for a small pressurized water reactor using an H infinity mixed sensitivity method. *Nuclear Engineering and Technology*. 2020 Jul;52(7):1443–51. https://doi.org/10.1016/j.net.2019.12.031
7. Dong Z. Nonlinear adaptive dynamic output-feedback power-level control of nuclear heating reactors. *Science and Technology of Nuclear Installations*. 2013;2013:794167. https://doi.org/10.1155/2013/794167
8. Etchepareborda A, Lolich J. Research reactor power controller design using an output feedback nonlinear receding horizon control method. *Nuclear Engineering and Design*. 2007 Feb;237(3):268–76. https://doi.org/10.1016/j.nucengdes.2006.04.002
9. Yun T, Su-Xia H, Chong L, Fu-Yu Z. An improved implicit multiple model predictive control used for movable nuclear power plant. *Nuclear Engineering and Design*. 2010 Oct;240(10):3582–5. https://doi.org/10.1016/j.nucengdes.2010.05.003
10. Wang G, Wu J, Zeng B, Xu Z, Wu W, Ma X. State-Space Model Predictive Control Method for Core Power Control in Pressurized Water Reactor *Nuclear Power Stations*. Nuclear Engineering and Technology. 2017 Feb;49(1):134–40. https://doi.org/10.1016/j.net.2016.07.008
11. Khajavi MN, Menhaj MB, Suratgar AA. A neural network controller for load following operation of nuclear reactors. [Online]. Available: www.elsevier.com/locate/anucene
12. Arab-Alibeik H, Setayeshi S. Adaptive control of a PWR core power using neural networks. *Annals of Nuclear Energy*. 2005 Apr;32(6):588–605. https://doi.org/10.1016/j.anucene.2004.11.004
13. Dong Z. A neural-network-based nonlinear adaptive state-observer for pressurized water reactors. *Energies*. 2013;6(10):5382–5401. https://doi.org/10.3390/en6105382
14. Dong Z. An artificial neural network compensated output feedback power-level control for modular high temperature gas-cooled reactors. *Energies*. 2014;7(3):1149–70. https://doi.org/10.3390/en7031149
15. Mousakazemi SMH, Ayoobian N, Ansarifar GR. Control of the reactor core power in PWR using optimized PID controller with the real-coded GA. *Annals of Nuclear Energy*. 2018 Aug;118:107–21. https://doi.org/10.1016/j.anucene.2018.03.038
16. Ansarifar GR, Saadatzi S. Sliding Mode Control for Pressurized-Water Nuclear Reactors in load following operations with bounded xenon oscillations. *Annals of Nuclear Energy*. 2015;76:209–17. https://doi.org/10.1016/j.anucene.2014.09.059
17. Hui J, Yuan J. Chattering-free higher order sliding mode controller with a high-gain observer for the load following of a pressurized water reactor. *Energy*. 2021 May;223:120066. https://doi.org/10.1016/j.energy.2021.120066
18. Vajpayee V, Becerra V, Bausch N, Deng J, Shimjith SR, Arul AJ. Robust-optimal integrated control design technique for a pressurized water-type nuclear power plant. *Progress in Nuclear Energy*. 2021 Aug;131:103575. https://doi.org/10.1016/j.pnucene.2020.103575
19. Abdulraheem KK, Korolev SA. Robust optimal-integral sliding mode control for a pressurized water nuclear reactor in load following mode of operation. *Annals of Nuclear Energy*. 2021 Aug;158:108288. https://doi.org/10.1016/j.anucene.2021.108288
20. Qiao L, Zhang W. Adaptive Second-Order Fast Nonsingular Terminal Sliding Mode Tracking Control for Fully Actuated Autonomous Underwater Vehicles. *IEEE Journal of Oceanic Engineering*. 2019 Apr;44(2):363–85. https://doi.org/10.1109/JOE.2018.2809018

21. Chen SY, Lin FJ. Robust nonsingular terminal sliding-mode control for nonlinear magnetic bearing system. *IEEE Transactions on Control Systems Technology*. 2011 May;19(3):636–43. https://doi.org/10.1109/TCST.2010.2050484

22. Kirgni HB, Wang J. LQR-based adaptive TSMC for nuclear reactor in load following operation. *Progress in Nuclear Energy.* 2023;156:1–11.

23. Kirgni HB, Wang J, Asif A. Static output feedback H∞ based integral sliding mode control law design for nuclear reactor power-level. *Progress in Nuclear Energy*. 2022;150:1–9.

24. Slotine JJ, Li W. Applied nonlinear control. Prentice Hall; 1991.

25. Spurgeon S. Sliding mode control: a tutorial. Proceedings of the 2014 European Control Conference (ECC 2014). 2014:2272–7. https://doi.org/10.1109/ECC.2014.6862622

26. Jiuwu H, Jingqi Y. Adaptive second-order nonsingular terminal sliding mode power-level control for nuclear power plants. *Nuclear Engineering and Technology*. 2021;54(5):1644–51.

27. Vajpayee V, Becerra V, Bausch N, Deng J, Shimjith SR, Arul AJ. L1-Adaptive Robust Control Design for a Pressurized Water-Type Nuclear Power Plant. *IEEE Transactions on Nuclear Science*. 2021 Jul;68(7).